Research Article | Vol. 29, No. 11 / 24 May 2021 / Optics Express 16563

Optics EXPRESS

28 GBd PAM-8 transmission over a 100 nm range using an InP-Si_3N_4 based integrated dual tunable laser module

DEVIKA DASS,[1,*] MARCOS TRONCOSO COSTAS,[1] LIAM P. BARRY,[1] SEAN O'DUILL,[1] CHRIS G. H. ROELOFFZEN,[2] DOUWE GEUZEBROEK,[2] GUILLERMO CARPINTERO,[3] ROBINSON CRUZOE GUZMAN,[3] AND COLM BROWNING[1]

[1]*School of Electronic Engineering, Dublin City University, Glasnevin, Dublin 9 D09 V209, Ireland*
[2]*LioniX International BV, 7521 AN Enschede, The Netherlands*
[3]*Carlos III de Madrid, Tecnología Electrónica Universidad, Leganés, Spain*
[*]*devika.dass2@mail.dcu.ie*

Abstract: This paper describes the detailed characterization of a novel InP-Si_3N_4 dual laser module with results revealing relative intensity noise (RIN) as low as −165 dB/Hz and wide wavelength tunability (100 nm). The hybrid coupled laser is deployed in an unamplified 28 GBd 8 level pulse amplitude modulation (PAM) short-reach data center (DC) transmission system. System performance, which is experimentally evaluated in terms of received signal bit error ratio (BER), demonstrates the ability of the proposed laser module to support PAM-8 transmission across a 100 nm tuning range with less than 1 dB variance in receiver sensitivity over the operating wavelength range. Comparative performance studies not only indicate that the proposed source can outperform a commercial external cavity laser (ECL) in an intensity modulation/direct detection (IM/DD) link but also highlight the critical impact of RIN in the design of advanced modulation short-reach systems.

1. Introduction

Recent technology advances, many of which rely on cloud computing platforms provided by DCs (e.g. ultra high definition video streaming, augmented reality), have led to significant increases in the demand for bandwidth by consumers. This demand, coupled with the growing pervasiveness of established cloud services such as tele-medicine, cloud storage and Internet of Things (IoT), is driving the continued evolution of data communications networks; for which the development of high capacity and spectrally efficient systems will be essential.

Currently, the IEEE P802.3db (400 GbE Task Force) standard is rapidly being deployed for short-reach fiber networks such as intra-DC links that can support bitrates of up to 400G, using coarse wavelength division multiplexing (CWDM) with eight wavelength channels each operating with PAM-4 at 50 Gbps [1]. Looking ahead, the Ethernet alliance roadmap indicates that the future link speeds are envisioned to be more than 1 Tb/s [2]. Considering the future proliferation of intra-DC interconnects, providing Terabit-scale operation across a DC network poses a major challenge. To address this issue of scalability, many works have highlighted the need to harness more spectrally efficient transmission technologies, as well the deployment of flexible networking in the optical domain using dynamic wavelength switching/routing (which overcomes the bandwidth limitations associated with current electronic switching technologies) [3,4].

While optical coherent solutions have recently been proposed in the literature [4,5], the associated cost of deployment may be prohibitive in the mid-term. Another option, which maintains the cost-effectiveness of (and provides a greater level of backward compatibility with)

#421929 https://doi.org/10.1364/OE.421929
Journal © 2021 Received 10 Feb 2021; revised 30 Apr 2021; accepted 9 May 2021; published 14 May 2021

Optics EXPRESS

today's systems, involves harnessing the spectral efficiency offered by dense WDM (DWDM) networking in the C-band in combination with PAM-8 transmission [6,7]. Due to the signal-to-noise ratio (SNR) requirements for PAM-8 transmission, a major hindrance to the development of transceivers in such DWDM IM/DD systems is the RIN of the optical source which limits performance [8]. Furthermore, the optical sources commonly used in DC transceivers (vertical cavity surface emitting lasers (VCSELs) and distributed feedback (DFB) lasers), do not exhibit wavelength tunability, making them incompatible with optical switching platforms which are predicated on transceiver wavelength versatility. Such proposed systems can exploit wavelength switching alone [9], or in tandem with optical space switching [10].

It is clear that in order to maximise DC network scalability afforded by a DWDM PAM platform, the development of a mass producible optical source - which supports higher order PAM transmission, exhibits flexibility in the optical domain and is compatible with surrounding integrated photonics - is critical. Optical devices based on photonic integration have shown the potential to be a key element of such evolved optical networks and have drawn a lot of attention in the recent years. Silicon photonic integrated circuits (PICs) are preferable to discrete semiconductor devices due to their compact size, high yield, and potentially lower cost [11]. The development of silicon-based optical sources in particular have the potential to enable fully integrated transceiver solutions and are the subject of much research with various approaches described in [12–14]. Outside of the SiP approach, compact laser designs such as the fiber Bragg grating (FBG)-based sources in [8] provide extremely low RIN (- 165 dBc/Hz), while the liquid crystal-based device in [15] gives full C-band tunability.

Recent works have examined the viability of PAM-8 transmission in short-reach IM/DD systems. Experiments in [6] target a data center interconnect (DCI) application, using an ECL to demonstrate 40 GBd PAM-8 transmission with the aid of a Volterra non-linear equalizer (VNLE) at the receiver. VCSELs have also been shown to support PAM-8 in some cases; with [16] demonstrating 28 GBd transmission over 25 km of single mode fiber (SMF) with the aid of injection locking/linear equalization (EQ), and [17] overcoming laser noise effects via transmitter side probabilistic shaping (PS) to achieve 33.3 GBd transmission in multi-mode fiber (MMF) system. The authors of [18] demonstrate 37.4 GBd PAM-8 transmission using a DFB in combination with a SiP modulator and frequency response EQ. The authors' previous works have proposed simplistic digital post-compensation for 56 GBd PAM-8 DCI transmission using an Electro Absorption Modulator (EAM) [19], and have demonstrated the use of a hybrid integrated micro-ring resonator (MRR) based tunable laser source for flexible PAM-4 short-reach systems [20].

In this work, a photonic integrated dual tunable laser module is shown to support 28 GBd PAM-8 transmission over an ultra-wide wavelength range of 100 nm using only simplistic digital signal processing (DSP) to achieve performance below the 7% forward error correction (FEC) limit. The discretely tunable device, which covers the entire C-band as well as part of the S-band, is comprised of two on-chip lasers, each of which is fabricated using hybrid coupling of an InP semiconductor optical amplifier (SOA) and a low loss Si_3N_4 feedback circuit. Device characterization reveals RIN values as low as −165 dB/Hz, and the evaluation of an IM/DD PAM-8 transmission system shows excellent performance across the operational range with a BER of 1.5×10^{-4} achieved over 1 km of SMF. A full description of the laser module, along with a detailed characterization, including wavelength tunability, output power, side mode suppression ratio (SMSR) and RIN is presented in section 2. The experimental setup is outlined in section 3, while section 4 presents the transmission results alongside performance analysis. Finally, section 5 concludes the work.

Optics EXPRESS

2. Description and characterization of the device

A schematic outline of the dual tunable laser module, shown in Fig. 1(a), consists of two lasers denoted as L1 and L2 (outlined in Fig. 1(a) in grey). Each laser consists of a gain, phase and cavity section along with associated 2×2 symmetric Mach-Zehnder Interferometer based tunable couplers (MZI-TC) [21] (labelled in Fig. 1(a) as cavity coupler (CC), PD/L1 output coupler (OC), PD/L2 OC). An additional MZI-TC (labelled in Fig. 1(a) as PD coupler) is used to control light to the photodetectors (PDs). The dual tunable laser was fabricated using two InP based reflective SOAs which are hybrid coupled to two Si_3N_4 feedback circuits. Both SOAs are designed to have the same gain spectra and support a wavelength range in excess of 100 nm. Each feedback circuit consists of two MRRs in a Vernier configuration, creating a MRR based external cavity laser (MRR-ECL). The phase section, the MRR and the MZI-TC are thermo-optically controlled with associated on-chip micro-heaters (highlighted in red in Fig. 1(a)). The hybrid assembly process used by the authors is described in the [22].

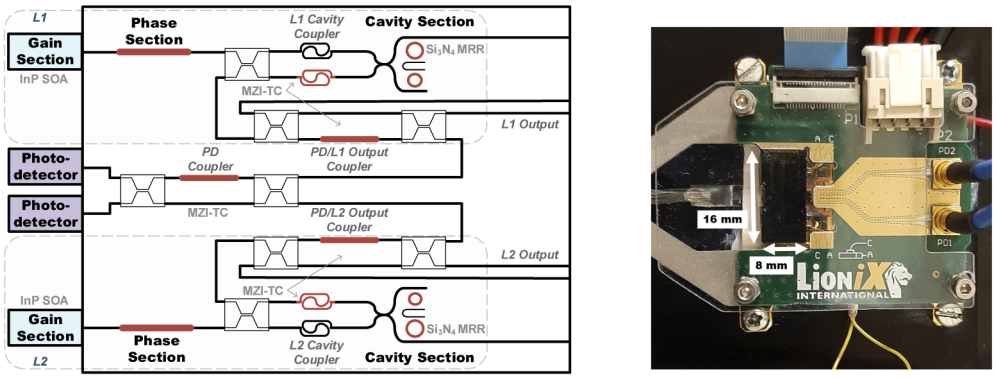

(a) PIC schematic

(b) Photograph

Fig. 1. Dual tunable InP-Si_3N_4 laser module

The SOA's left facet is coated with high reflective material to reduce cavity losses and the right facet is coated with low reflective material to facilitate lasing in the external cavity [23,24]. The PIC consists of two Si_3N_4 feedback circuits, each incorporating a pair of MRRs. Both pairs of MRRs on the chip exhibit circumferences of 787.119 μm and 813.336 μm, and free spectral ranges (FSRs) of 1.7242 nm and 1.668 nm respectively. The Si_3N_4 waveguides, having a symmetric double-stripe cross section, offer a low propagation loss of about 0.1 dB/cm [22], which allows the MRRs to reach Q-factors ranging from 20000 to 200000 [25]. The multiple round-trips through the two MRRs, yield a longer low loss cavity length and a narrower spectral filtering of the wavelength, producing a single mode output [22]. Tuning of the single mode output can be achieved by varying the voltage of the micro-heater associated with each ring. The amount of light fed back to the gain and cavity sections of a laser is controlled by the thermally adjustable phase section and cavity coupler. The light from lasers L1 and L2 is directed to couplers PD/L1 and PD/L2 respectively, where the relative light power directed to either the on-chip detectors or output fibers can be set. Finally, the on-chip photodiodes include a PD coupler, which controls the power level that is coupled to each PD. The PDs can be used for power monitoring or to enable optical heterodyne operation whereby the interaction of the two lasers on a diode produces a high frequency carrier (mmWave/ terahertz) which can be used for optical/wireless applications. A photograph of the InP-Si_3N_4 hybrid integrated dual laser module is shown in Fig. 1(b). As shown in the image, the optical waveguide access ports are coupled to

Optics EXPRESS

single mode polarization maintaining fibers, which are terminated with an angled facet FC/APC connector.

For the characterization of the device, the temperature of the laser module was maintained at room temperature (20°C) using a laser diode thermoelectric cooler (TEC) connected to the temperature sensor IC inserted in the module. Each laser was operated one at a time for individual characterization. The gain current for both the lasers was set to 100 mA. For the purposes of observing the effects of tuning the MRRs in the feedback circuit, the phase sections and the cavity coupler sections were biased at 0 V throughout the characterization. The voltage of the micro-heater associated with the PD/L1 and PD/L2 output couplers were kept constant at 15 V to maximize optical power from the fiber output of individual laser for the above bias settings. For each laser on the chip the tuning map and the SMSR, shown in Fig. 2, were obtained by observing the output wavelength characteristics using an optical spectrum analyzer (OSA) while varying the voltage applied to the micro-heaters associated with the two MRRs. The fine tuning was achieved by changing the voltage of both the rings by small values within the range of 0 V to 10 V with a step size of 0.1 V.

The dual laser module's wavelength tuning maps, presented in the Figs. 2(a) and (b), show the tuning ranges for L1 (from 1470 nm to 1540 nm) and L2 (from 1510 nm to 1575 nm), respectively. This reduction in coverage (with respect to that supported by both SOAs) and the difference in wavelength ranges exhibited by L1 and L2 are attributed to the respective spectral dependencies of the cavity coupler MZI-TCs [26], which were biased at 0 V during characterization. Altering these bias conditions allows the lasers' wavelength coverage to be tuned. For the settings used for characterization, the dual laser module exhibits a tuning range of 100 nm, covering most of the S band and all of the C band. Figures 2(c) and (d) show that an SMSR of greater than 50 dB is achieved across the whole range of wavelengths for the gain and bias settings used during this characterization. However, by increasing the gain currents, and fine tuning the MZI-TCs, a further increase in the output power up to +10 dBm can be achieved on both laser outputs. The fiber coupled output powers of L1 and L2 as a function of gain current (with all other bias settings fixed) which were measured independently and are shown in Figs. 2(e) and (f). Figure 2(e) shows the power-current (P-I) curves when the heaters associated with each lasers' output coupler and cavity coupler MZI-TCs were biased at 15 V and 0 V respectively (the conditions used for wavelength and SMSR characterization), while Fig. 2(f) shows P-I curves when these bias conditions were set to maximize the output power at higher gain currents. The power drops exhibited by all P-I curves are explained by the fact that while the biasing configurations in the external cavities remain constant, increasing the gain current results in refractive index changes in the gain waveguide; serving to slightly shift the lasing mode out of resonance with the MRR-based Vernier filter [22]. Figure 2(e) shows threshold currents for L1 and L2 of 29 mA and 10 mA respectively. While biasing conditions do impact on the threshold current, this relatively large variation between L1 and L2 is attributed to differences in chip-to-chip coupling losses, and potentially to small differences in respective SOA reflectivities. This loss also impacts upon the maximum achievable output power for both lasers. Nevertheless, Fig. 2(f) shows that powers > +10 dBm can be achieved using both L1 and L2 through suitable tuning of the output coupler and cavity coupler MZI-TCs. Figures 2(c) and (f) show some regions which indicate deteriorations in both SMSR and output power. These regions arise at MRR bias settings for which the oscillating cavity mode is off-resonance with the Vernier filter to some degree. In some cases, this deterioration could be alleviated by appropriate tuning of the phase sections. The optical spectra corresponding to a selection of wavelengths across the device's full tuning range (about 100 nm) are superimposed and presented in Fig. 3.

As mentioned previously, RIN is a limiting factor which plays a critical role in the performance of IM/DD systems employing digital multi-level signaling. The laser noise RIN measurements were performed using a method similar to that outlined in Ref. [24]. In the RIN measurement

Optics EXPRESS

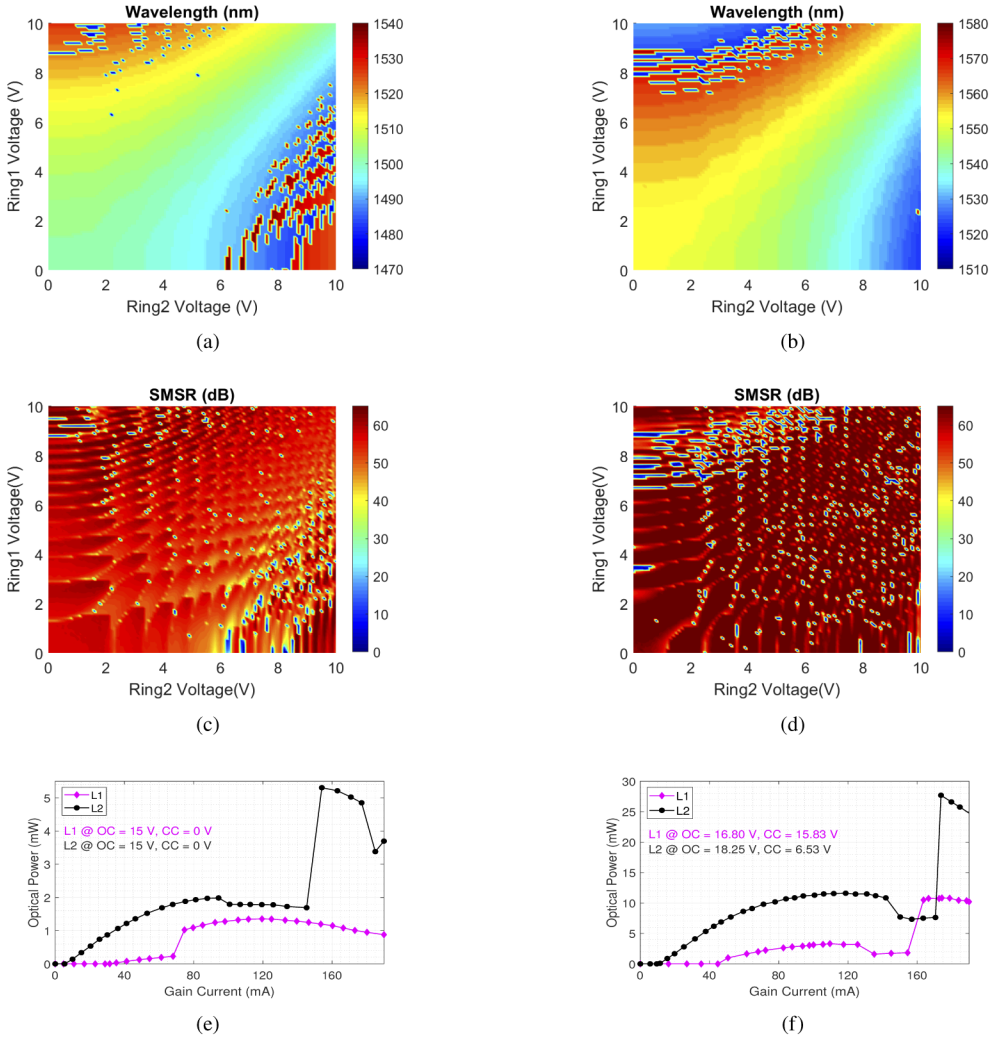

Fig. 2. (a), (b) Tuning map of the wavelength versus voltage on the ring section for L1 and L2 respectively. (c), (d) SMSR versus voltage on the ring sections for L1 and L2 respectively. (e), (f) Optical power of L1 and L2 versus gain current with bias conditions of the MZI-TCs given in the inset.

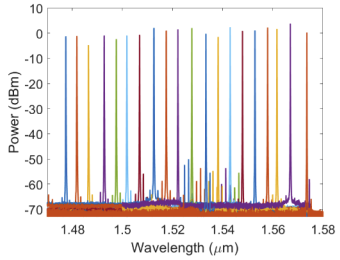

Fig. 3. Superimposed spectra of L1 and L2 over 100 nm tuning range.

Optics EXPRESS

setup, the output of the laser was fed into a high bandwidth (~20 GHz) Thorlabs DXM20AF PD with an inbuilt bias tee and an impedance-matching circuit. The AC signal was amplified using an SHF 806E electrical amplifier and fed to a Rohde & Schwarz FSW50 electrical spectrum analyser (ESA) to measure the power across the 0 GHz to 20 GHz frequency band. A selection of measured RIN profiles across the 100 nm tuning range of the dual tunable device is shown in Fig. 4. For all wavelengths, low frequency RIN below 2.5 GHz, does not exceed −153 dB/Hz, while at higher frequencies up to 20 GHz, RIN reduces to values within the range of −160 dB/Hz to −165 dB/Hz.

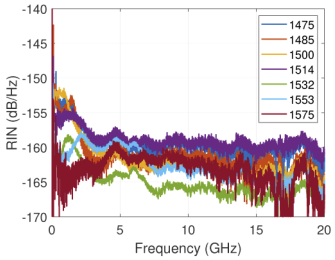

Fig. 4. RIN measured RIN at different wavelengths.

3. Experimental setup for PAM-8 transmission

The short-reach PAM-8 experimental setup is shown in Fig. 5. Using the tuning maps presented in the previous section, the tuning sections of each laser were optimized to obtain an optical carrier with the desired wavelength, power and SMSR. L1 was used to generate wavelengths in the S-band and L2 was used to generate wavelengths in the C-band, with roughly 10 dBm output power achieved for all operating wavelengths. To achieve this output power the gain currents of L1 and L2 were set to the to 170 mA and 100 mA respectively, as depicted in Fig. 2(f).

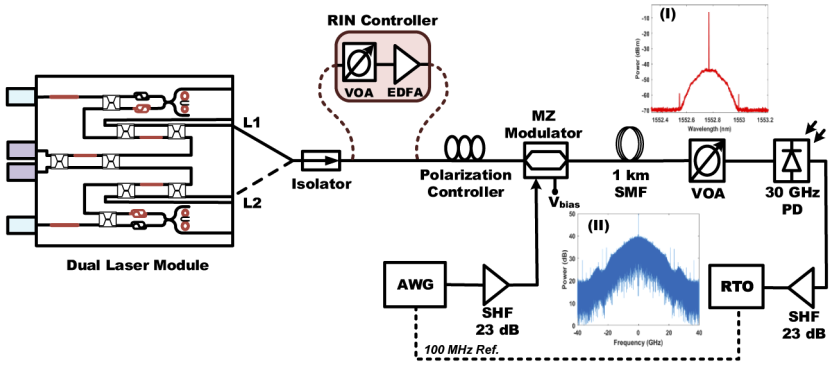

Fig. 5. Experimental setup showing the switching between L1 and L2 of the dual module laser. The inset (I) shows optical spectrum of PAM-8 signal at PD and (II) shows electrical spectrum of PAM-8 signal at RTO.

A pseudorandom PAM-8 signal of length 2^{15} symbols was generated offline using MATLAB. The PAM signal was then predistorted through symbol level adjustment in order to compensate for the non-linear transfer function of the Sumitomo 40 GHz single ended $LiNbO_3$ Mach-Zehnder modulator (MZM) used. The 28 GBaud PAM-8 electrical signal was generated by the Keysight M9502A arbitrary waveform generator (AWG) operating at 84 GSa/s and amplified before driving

Optics EXPRESS

the MZM which was biased at quadrature. The output voltage of the AWG, as well as the gain on the linear amplifier, were carefully selected to obtain the MZM drive voltage required to maximize the extinction of the transmitted optical PAM-8 signal. After modulation of the optical carrier via the MZM, the signal was transmitted through 1 km of SMF. At the receiver, a variable optical attenuator (VOA) was used to vary the received optical power falling on a 30 GHz PIN PD. The obtained photocurrent was amplified to allow its capture, at a sample rate of 100 GSa/s, with the Tektronix DPO77002SX real time oscilloscope (RTO).

In order to examine the limitations imposed by RIN in the PAM-8 transmission system, an optical source with variable RIN level was synthesized. This was achieved by connecting the output of L2 (operating at 1553 nm) to an EDFA through a VOA, shown as RIN controller in Fig. 5. By setting the EDFA to have a fixed output power of +10 dBm, the input optical carrier power can be varied by the VOA, thus producing relative changes in the amplitude noise exhibited by the output optical carrier. This allowed the RIN of the output optical carrier to be precisely controlled while maintaining constant lasing conditions. For further comparisons, an ECL tuned to operate at 1553 nm was also used as a transmitter source for performance evaluation. The received signal was digitally processed offline with different steps including resampling, normalization, equalization, symbol synchronization and PAM-8 decoding. A decision-directed least-mean square (DD-LMS) algorithm was used to train the weights of a 21-tap adaptive filter. After processing, the BER was calculated by counting errors over several captured bit sequences.

4. Results and discussion

The unamplified short-reach PAM-8 system outlined was evaluated in terms of BER with respect to the received optical power (ROP) using a selection of wavelengths from the dual laser module spanning the full 100 nm range. The results after 1 km of SMF, presented in Fig. 6(a), show that in all cases the measured BER was below the 7% FEC limit (3×10^{-3}) for received optical powers greater than −7 dBm. Less than 1 dB of variability in received power was found across the whole spectrum for any given BER. The consistency of this performance across an extremely wide tuning range, highlights the potential of the dual mode laser for flexible short reach communications. Using L2 at 1553 nm, three optical carriers of wavelength, denoted by λ, at 1553 nm with different RIN values were obtained by changing the input power into the 'RIN controller' EDFA while keeping a constant output power, resulting in variable levels of gain and amplified spontaneous emission (ASE) from the EDFA. The RIN of each configuration was measured using the process outlined in section 2. For the cases where RIN was varied using the EDFA with total gains of 20 dB, 24 dB and 29 dB, the obtained RIN values were −144 dB/Hz, −140 dB/Hz and −135 dB/Hz, respectively. The RIN value for the ECL employed in the experiments was −155 dB/Hz. Fig. 6(b) shows BER versus ROP for each source RIN level evaluated in the short-reach PAM-8 system. In the figure, 'L2' denotes the use of the hybrid laser module alone, while 'L2+EDFA' denotes the use of the hybrid laser module in conjunction with the 'RIN controller' EDFA to obtain the various RIN levels, as described above. The figure shows that while all carriers exhibit similar performances at lower ROPs (due to the impact of receiver thermal noise), transmission with carrier RIN levels of −144 dB/Hz, −140 dB/Hz and −135 dB/Hz results in the emergence of error floors at higher ROPs as RIN becomes the dominant noise process. This highlights the critical impact of RIN on the performance of higher order PAM IM/DD systems. The figure shows that these error floors are alleviated through the use of the low RIN carriers provided by L2 (−160 dB/Hz) and the ECL (−155 dB/Hz). For these RIN levels, [8] confirms that receiver shot noise is in fact the dominant noise process at a ROP of −4 dBm, and in fact this would be the case for received powers in the range of +3 dBm to +5 dBm (neglecting potential non-linearities due to the PD). Overall, the superior low noise performance exhibited by the MRR-based hybrid integrated device results in a 3 dB improvement in the receiver sensitivity as compared to the worst case RIN presented (−135 dB/Hz) at the FEC limit. The results also show how the device

Optics EXPRESS

outperforms a commercial ECL, exhibiting a 0.5 dB improvement in receiver sensitivity at BERs below 1×10^{-3}.

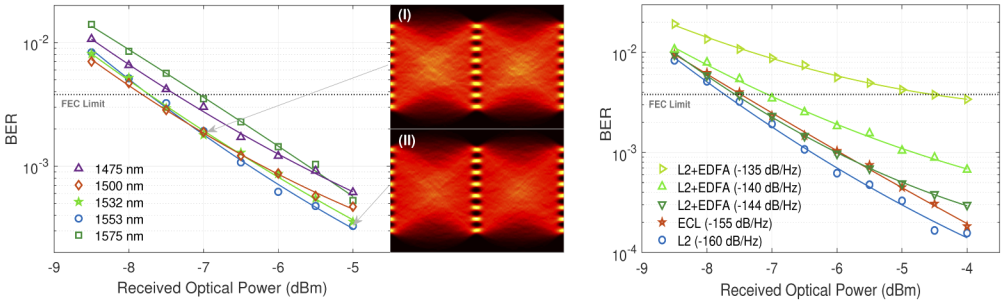

Fig. 6. (a) BER versus ROP for various wavelengths after 1 km of SMF. (I) Eye diagram for λ=1553 nm at −7 dBm ROP. (II) Eye diagram for λ=1553 nm at −5 dBm ROP. (b) BER vs ROP for different RIN levels for λ=1553 nm after 1 km of SMF.

5. Conclusion

With the ongoing increase in bandwidth requirements driven by many internet applications, there is a drive to enhance the capacity and cost effectiveness of short reach DC interconnects. Optical integration will play a key role in the development of cost effective links as many transmitters and modulators can be integrated on a single chip. Ensuring these optical transmitters have the required noise levels to handle multi-level signaling is also vital for the deployment of spectrally efficient PAM-N formats. This work has presented an integrated dual laser source which can be tuned over 100 nm while maintaining the SMSR over 50 dB and the RIN values around −160 dB/Hz. Using both lasers in tandem can provide two wavelengths with up-to 70 nm tunability each, while combining the fiber outputs allows for a single wavelength operation over the module's full tuning range. The device is shown to be capable of supporting unamplified short-reach PAM-8 transmission over its entire wavelength range, while maintaining the requirement for low complexity DSP.

Overall, the potential for mass production of the PIC-based design approach, the compatibility with surrounding electronic/optical silicon technologies and the facilitation of highly spectrally efficient IM/DD transmission, point toward to the ability of the presented InP-Si_3N_4 dual laser to be a key component in a wider cost-efficient and scalable DWDM solution for future DC networks.

Funding. Science Foundation Ireland (12/RC/2276_P2, 13/RC/2077_P2, 16/RI/3698, 18/EPSRC/3591, 18/SIRG/5579).

Acknowledgments. We thank Dr. Yi Lin for assistance with the initial characterization of the device.

Disclosures. The authors declare no conflicts of interest.

References

1. IEEE P802.3bs 400 Gb/s Ethernet Task Force [Online]. Available = https://www.ieee802.org/3/index.html.
2. 2020 Roadmap - Ethernet Alliance. Available = https://ethernetalliance.org/technology/2020-roadmap/.
3. Q. Cheng, M. Bahadori, M. Glick, S. Rumley, and K. Bergman, "Recent advances in optical technologies for data centers: a review," Optica **5**(11), 1354–1370 (2018).
4. X. Zhou, R. Urata, and H. Liu, "Beyond 1 Tb/s Intra-Data Center Interconnect Technology: IM-DD OR Coherent?" J. Lightwave Technol. **38**(2), 475–484 (2020).
5. M. Morsy-Osman, M. Sowailem, E. El-Fiky, T. Goodwill, T. Hoang, S. Lessard, and D. V. Plant, "DSP-free 'coherent-lite' transceiver for next generation single wavelength optical intra-datacenter interconnects," Opt. Express **26**(7), 8890–8903 (2018).

Optics EXPRESS

6. D. Zou, F. Li, Z. Li, W. Wang, Q. Sui, Z. Cao, and Z. Li, "100G PAM-6 and PAM-8 Signal Transmission Enabled by Pre-Chirping for 10-km Intra-DCI Utilizing MZM in C-band," J. Lightwave Technol. **38**(13), 3445–3453 (2020).
7. H. Liu, R. Urata, X. Zhou, and A. Vahdat, "Evolving Requirements and Trends of Datacenters Networks,", in *Springer Handbook of Optical Networks*, (Springer, 2020), pp. 707–724.
8. P. A. Morton and M. J. Morton, "High-Power, Ultra-Low Noise Hybrid Lasers for Microwave Photonics and Optical Sensing," J. Lightwave Technol. **36**(21), 5048–5057 (2018).
9. H. Ballani, P. Costa, R. Behrendt, D. Cletheroe, I. Haller, K. Jozwik, F. Karinou, S. Lange, K. Shi, B. Thomsen, and H. Williams, "Sirius: A Flat Datacenter Network with Nanosecond Optical Switching," (Association for Computing Machinery, New York, NY, USA, 2020), SIGCOMM '20, p. 782–797.
10. A. Gazman, C. Browning, M. Bahadori, Z. Zhu, P. Samadi, S. Rumley, V. Vujicic, L. P. Barry, and K. Bergman, "Software-defined control-plane for wavelength selective unicast and multicast of optical data in a silicon photonic platform," Opt. Express **25**(1), 232–242 (2017).
11. P. Dong, Y.-K. Chen, G.-H. Duan, and D. T. Neilson, "Silicon photonic devices and integrated circuits," Nanophotonics **3**(4-5), 215–228 (2014).
12. A. Abbasi, J. Verbist, L. A. Shiramin, M. Verplaetse, T. De Keulenaer, R. Vaernewyck, R. Pierco, A. Vyncke, X. Yin, G. Torfs, G. Morthier, J. Bauwelinck, and G. Roelkens, "100-Gb/s Electro-Absorptive Duobinary Modulation of an InP-on-Si DFB Laser," IEEE Photonics Technol. Lett. **30**(12), 1095–1098 (2018).
13. S. Chen, W. Li, J. Wu, Q. Jiang, M. Tang, S. Shutts, S. N. Elliott, A. Sobiesierski, A. J. Seeds, I. Ross, P. M. Smowton, and H. Liu, "Electrically pumped continuous-wave III-V quantum dot lasers on silicon," Nat. Photonics **10**(5), 307–311 (2016).
14. B. R. Koch, E. J. Norberg, B. Kim, J. Hutchinson, J.-H. Shin, G. Fish, and A. Fang, "Integrated silicon photonic laser sources for telecom and datacom," in *2013 Optical Fiber Communication Conference and Exposition and the National Fiber Optic Engineers Conference (OFC/NFOEC)*, (2013), pp. 1–3.
15. J. De Merlier, K. Mizutani, S. Sudo, K. Naniwae, Y. Furushima, S. Sato, K. Sato, and K. Kudo, "Full c-band external cavity wavelength tunable laser using a liquid-crystal-based tunable mirror," IEEE Photonics Technol. Lett. **17**(3), 681–683 (2005).
16. Y. C. Wang, H. H. Lu, C. Y. Li, P. H. Chew, Y. B. Jheng, W. S. Tsai, and X. H. Huang, "A high-speed 84 gb/s vsb-pam8 vcsel transmitter-based fiber–ivllc integration," IEEE Photonics J. **10**(5), 1–8 (2018).
17. L. Sun, C. Wang, J. Du, C. Liang, W. Zhang, K. Xu, F. Zhang, and Z. He, "Dyadic probabilistic shaping of PAM-4 and PAM-8 for cost-effective VCSEL-MMF optical interconnection," IEEE Photonics J. **11**(2), 1–11 (2019).
18. M. Chagnon, M. Osman, M. Poulin, C. Latrasse, J. F. Gagné, Y. Painchaud, C. Paquet, S. Lessard, and D. Plant, "Experimental study of 112 Gb/s short reach transmission employing PAM formats and SiP intensity modulator at 1.3 μm," Opt. Express **22**(17), 21018–21036 (2014).
19. C. Browning, M. Ruffini, B. Cardiff, and L. P. Barry, "Single lane 168 gb/s pam-8 short reach transmission using an eam with receiver skew compensation," in *2018 European Conference on Optical Communication (ECOC)*, (IEEE, 2018), pp. 1–3.
20. C. Browning, M. Ruffini, Y. Lin, R. B. Timens, D. H. Geuzebroek, C. G. H. Roeloffzen, D. Geskus, R. M. Oldenbeuving, R. G. Heideman, Y. Fan, K. J. Boller, and L. P. Barry, "Optically switched 56 GBd PAM-4 using a hybrid InP-TriPleX integrated tunable laser based on silicon nitride micro-ring resonators,"in *2018 Conference on Lasers and Electro-Optics (CLEO)*, (IEEE, 2018), pp. 1–2.
21. C. G. Roeloffzen, L. Zhuang, C. Taddei, A. Leinse, R. G. Heideman, P. W. van Dijk, R. M. Oldenbeuving, D. A. Marpaung, M. Burla, and K.-J. Boller, "Silicon nitride microwave photonic circuits," Opt. Express **21**(19), 22937–22961 (2013).
22. C. G. H. Roeloffzen, M. Hoekman, E. J. Klein, L. S. Wevers, R. B. Timens, D. Marchenko, D. Geskus, R. Dekker, A. Alippi, R. Grootjans, A. van Rees, R. M. Oldenbeuving, J. P. Epping, R. G. Heideman, K. Worhoff, A. Leinse, D. Geuzebroek, E. Schreuder, P. W. L. van Dijk, I. Visscher, C. Taddei, Y. Fan, C. Taballione, Y. Liu, D. Marpaung, L. Zhuang, M. Benelajla, and K.-J. Boller, "Low-Loss Si_3N_4 TriPleX Optical Waveguides: Technology and Applications Overview," IEEE J. Select. Topics Quantum Electron. **24**(4), 1–21 (2018).
23. J. P. Epping, A. Leinse, R. M. Oldenbeuving, I. Visscher, D. Geuzebroek, D. Geskus, A. van Rees, K. J. Boller, M. Theurer, M. Möhrle, C. G. Roeloffzen, and R. G. Heideman, "Hybrid integrated silicon nitride lasers," in *Physics and Simulation of Optoelectronic Devices XXVIII*, vol. 11274 (International Society for Optics and Photonics, 2020), p. 112741L.
24. Y. Lin, C. Browning, R. B. Timens, D. H. Geuzebroek, C. G. Roeloffzen, M. Hoekman, D. Geskus, R. M. Oldenbeuving, R. G. Heideman, Y. Fan, K. J. Boller, and L. P. Barry, "Characterization of hybrid inp-triplex photonic integrated tunable lasers based on silicon nitride (Si_3N_4/SiO_2) microring resonators for optical coherent system," IEEE Photonics J. **10**(3), 1–8 (2018).
25. Y. Fan, R. M. Oldenbeuving, C. G. H. Roeloffzen, M. Hoekman, D. Geskus, R. G. Heideman, and K.-J. Boller, "290 hz intrinsic linewidth from an integrated optical chip-based widely tunable inp-si3n4 hybrid laser," in *2017 Conference on Lasers and Electro-Optics (CLEO)*, (2017), pp. 1–2.
26. K.-J. Boller, A. van Rees, Y. Fan, J. Mak, R. E. M. Lammerink, C. A. A. Franken, P. J. M. van der Slot, D. A. I. Marpaung, C. Fallnich, J. P. Epping, R. M. Oldenbeuving, D. Geskus, R. Dekker, I. Visscher, R. Grootjans, C. G. H. Roeloffzen, M. Hoekman, E. J. Klein, A. Leinse, and R. G. Heideman, "Hybrid Integrated Semiconductor Lasers with Silicon Nitride Feedback Circuits," Photonics **7**, 4 (2020).